Chapter 9

Stresses on Expansion Joints Used in Penetrations

Chapter details

Chapter DOI:

https://doi.org/10.4322/978-65-86503-83-8.c09

Chapter suggested citation / reference style:

Suanno, Rodolfo, Maneschy, José E. (2022). "Stresses on Expansion Joints Used in Penetrations". *In* Jorge, Ariosto B., et al. (Eds.) *Fundamental Concepts and Models for the Direct Problem*, Vol. II, UnB, Brasilia, DF, Brazil, pp. 231–259. Book series in Discrete Models, Inverse Methods, & Uncertainty Modeling in Structural Integrity.

P.S.: DOI may be included at the end of citation, for completeness.

Book details

Book: Fundamental Concepts and Models for the Direct Problem

Edited by: Jorge, Ariosto B., Anflor, Carla T. M., Gomes, Guilherme F., & Carneiro, Sergio H. S.

Volume II of Book Series in:

Discrete Models, Inverse Methods, & Uncertainty Modeling in Structural Integrity

Published by: UnB City: Brasilia, DF, Brazil Year: 2022

DOI: https://doi.org/10.4322/978-65-86503-83-8

Stresses on Expansion Joints Used in Penetrations

Rodolfo Suanno[1*], José Eduardo Maneschy[2]

[1]Stress Analysis Department - DAN.T, Eletrobras Eletronuclear – Rio de Janeiro, Brazil. E-mail: rsuanno@eletronuclear.gov.br/rsuanno@gmail.com
[2]JEM Consultoria. E-mail:emanesc@gmail.com

*Corresponding author

Abstract

During the 8th outage of the Angra 2 power plant, the expansion joints of the containment penetration JMK05D0201 (LCQ50) were found distorted. The cause was an inadvertent over pressurization made during monthly tests to verify the set pressure. To leave the damaged expansion joint installed, Eletronuclear conducted an elastic-plastic analysis which has demonstrated its integrity. Eletronuclear decided to keep it in place and cover it with an expansion joint designed to resist all loads predicted in the original design specification. This new design is a two-sided (bipartite) bellows with longitudinal field welds. This chapter presents the fatigue and stress analysis of the bipartite overlapping expansion joints considering the loads defined in the design specification.

Keywords: expansion joints; stress analysis; fatigue, mechanical penetrations.

1 Introduction

In nuclear power plants expansion joints, also known as bellows, are frequently mounted in penetrations of the metal containment whose function is to maintain the sealing of the reactor building in case of an accident due to loss of primary refrigerant (LOCA – Loss of Coolant Accident). The joints are designed to absorb the pressure stresses and thermal displacements from the heating and cooling that occur during the operation of the systems where they are installed. The project also includes other loads, such as pressure tests, seismic movements, and LOCA.

During the Angra 2 outage held in 2010, the penetration expansion joints JMK05D0201 (LCQ50) were found distorted, as shown in Figure 1. The cause of the observed deformation was excessive over-pressurization that was inadvertently imposed on the joints during the tests performed periodically to verify their water tightness. As this request was not foreseen, compression instability and subsequent buckling, known in the specialized literature as squirm, of the part occurred.

The evaluations carried out by the construction and engineering teams concluded that replacing the distorted joints with new ones would be extremely complex. Thus, Eletronuclear decided to leave them in service, and install another expansion joint overlapping each of them, designed to resist the same loads specified in the original design. The new configuration, installed in 2011, is a double joint, formed by two similar pieces, connected using a longitudinal weld performed during its assembly in the field.

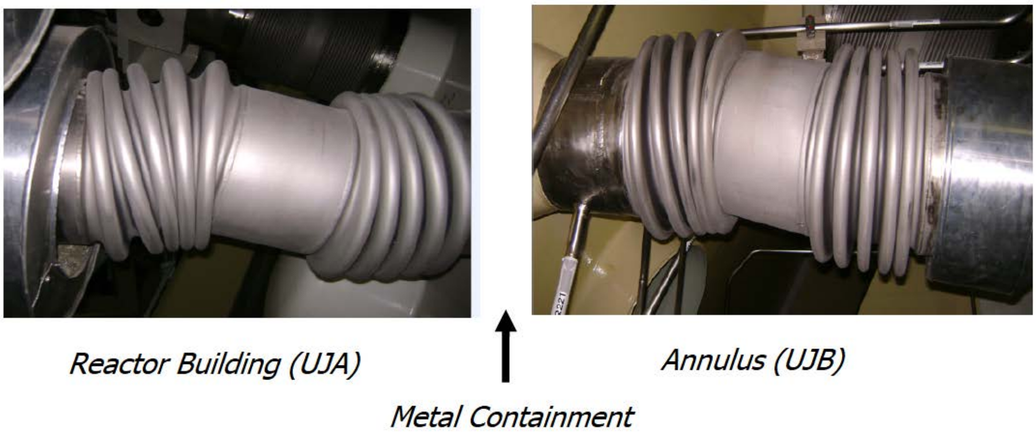

Figure 1 - Distorted penetration expansion joints (LCQ50) of the steam generator purge system

The expansion joints under study belong to the steam generator purge system (LCQ). In each of its loops, this system has two joints connected to the penetration (or nozzle) of the containment shell, one on the side of the reactor building, the UJA, and the other in the annulus, the UJB observed in Figure 2 and 3. A fixed point inside the containment isolates the pipe joints from the purge system. As the double pipe, called the guard pipe, which protects containment in case of breakage of the process line, is fastened directly at the fixed point, there is no load transfer generated by the movements of the containment to the pipe.

In this work, the stress and fatigue analysis is carried out to demonstrate that the configuration with the overlapping joint is adequate from the structural point of view. The evaluation is made by comparing the permissible limits of the codes and standards with the values calculated using loads of the original design, which are the internal pressure and thermal displacements in normal/abnormal operating conditions, the pressure during periodic tests, and displacements caused by LOCA and during the earthquake of safe shutdown plus burst pressure wave. In the present case, the ASME code Section III Subsection NB, and the standard AD-2000/B13 were adopted for stress and fatigue checks, respectively.

The stresses and deformations were determined by the finite element method, with the analyses made in ANSYS and conducted in an elastic regime for the operation load cases, and elastoplastic for tests and accidents. The model uses shell elements to simulate the joint, the tube between the bellows, and the double guard pipe. Contact elements are used to simulate the interaction between bellows.

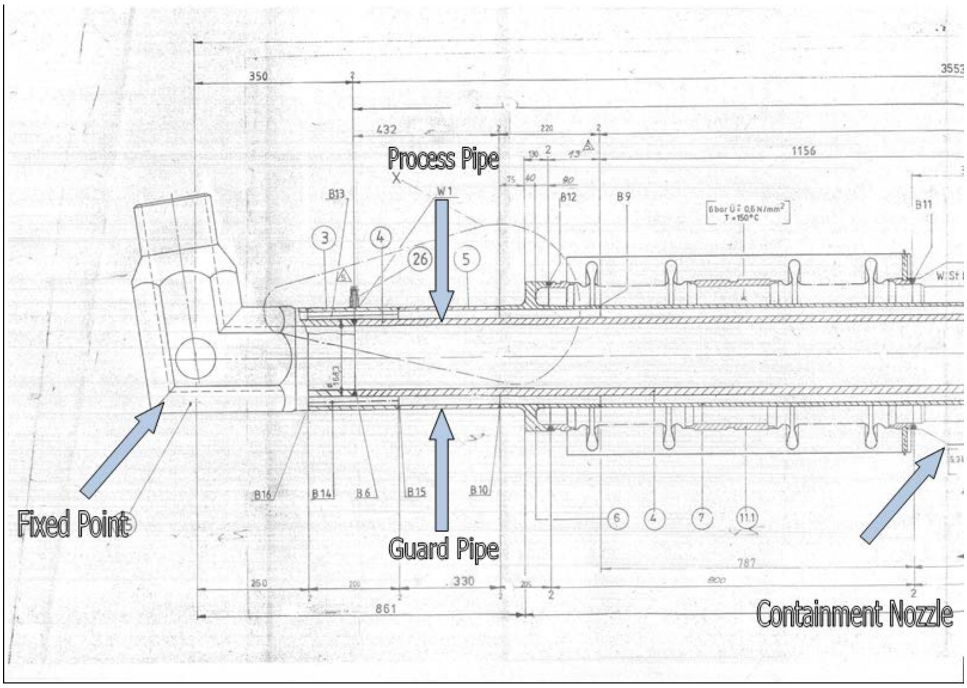

Figure 2- Penetration of the steam generator purge system (UJA building)

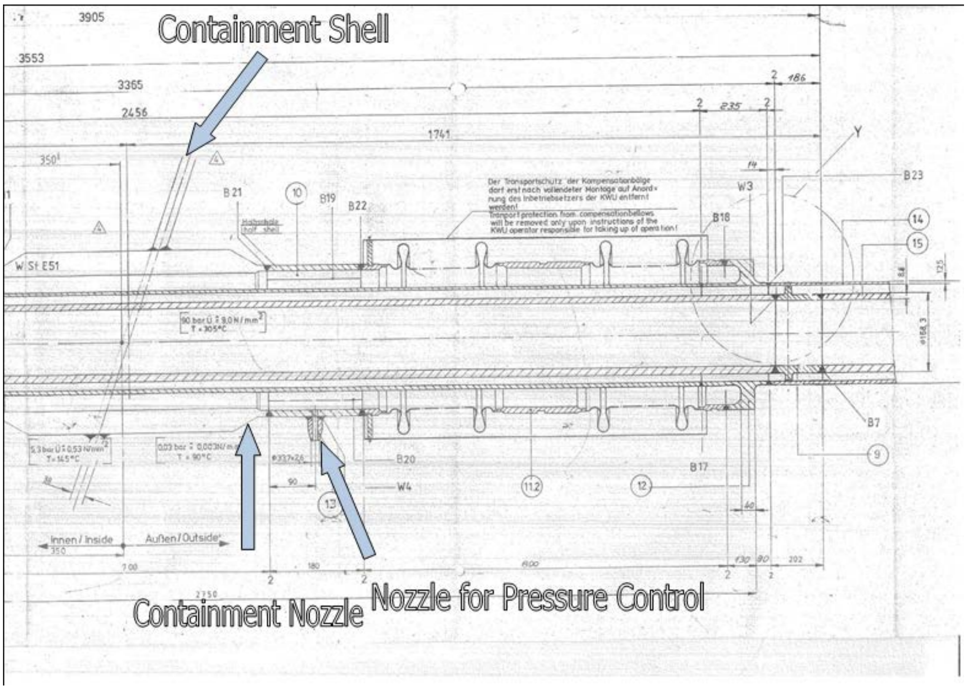

Figure 3- Penetration of the steam generator purge system (UJB building)

2 Original and overlapping expansion joint

The original configuration of the JMK05D0201 penetration expansion joint is universal, with one layer, without reinforcement, five convolutions in each bellow, and consisting of two joints connected by a cylindrical section tube, as illustrated in Figures 4 and 5. The joint was built to specification and manufactured from stainless steel X10CrNiNb18 9 (1.4550).

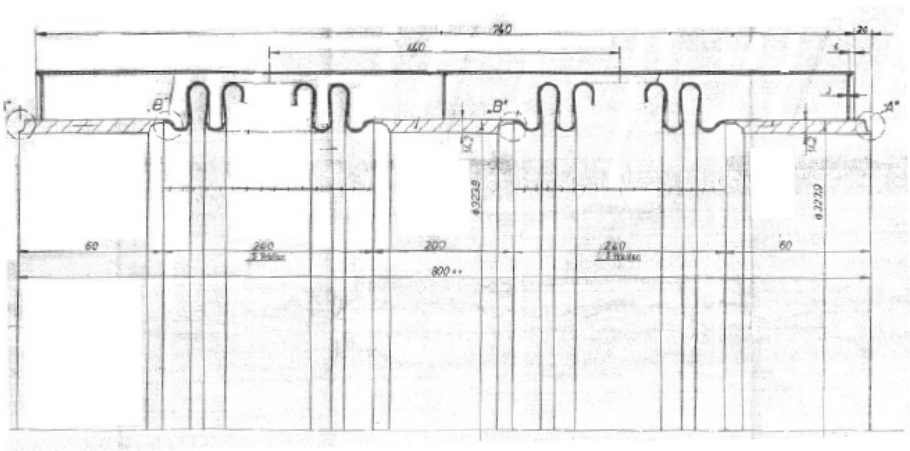

Figure 4- Original expansion joint

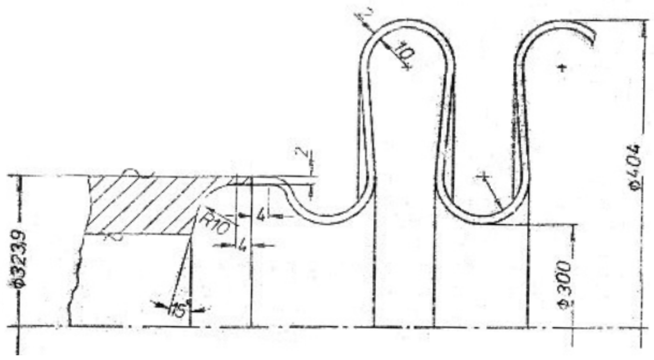

Figure 5 – Original expansion joint. Convolution geometry detail (dimensions in mm)

The overlapping expansion joint is bipartite, consisting of two identical half parts, which are connected by longitudinal welding made during assembly in the field. The representations in Figure 6 show the geometric details of the piece. The specifications, standards, and material for its manufacture are the same as the original joint.

3 Finite element model

As mentioned in Section 1, in each loop of the steam generator purge system there are two expansion joints, one attached to the inner side of the containment in the reactor building (UJA), and on the outside side, in the annulus (UJB). The loads on the joints are the internal pressure between them and the guard pipe, the thermal displacements of operation transmitted by the guard pipe, and the movements imposed by the containment nozzle during tests and accidents. For all these loadings the influence of the flexibility of the region between the fixed point and the expansion joint is negligible. Consequently, only one of them will be modeled since the interest is on the stresses acting in the expansion joint and guard pipe in the overlapping region.

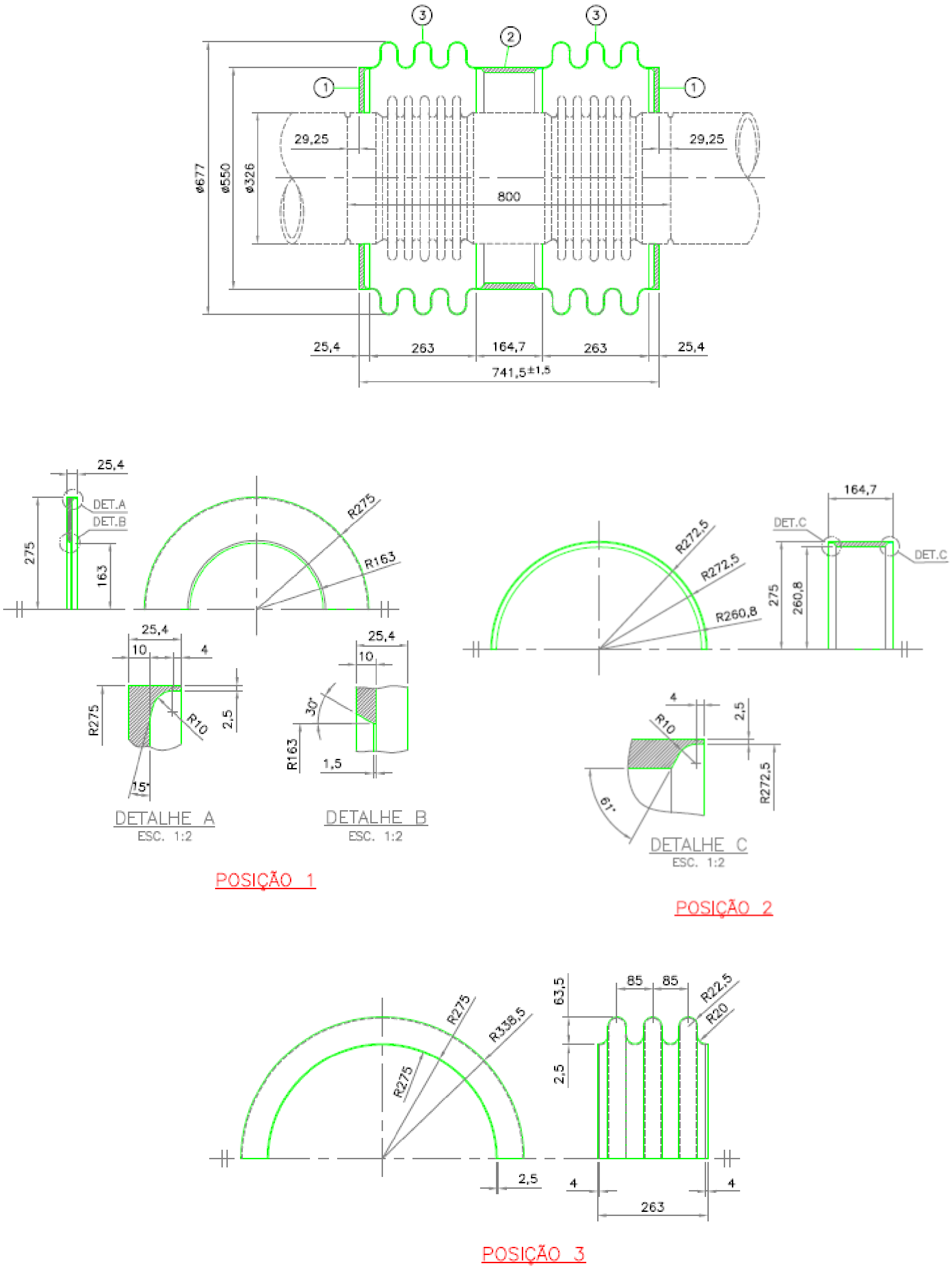

Figure 6 - Overlapping expansion joint (dimensions in mm)

Two finite element models were developed, one to simulate the original joint alone and the other to represent the original joint plus the overlapping. The expansion joint and guard pipe are modeled by SHELL281 shell elements (quadratic interpolation function) of the ANSYS program. By simplification, the part of the guard pipe that extends from the expansion joint to the supports (fixed point on one side and containment nozzle on the other), is modeled with PIPE16 beam elements. The transition between the shell and beam elements that simulate the continuity of the guard pipe is done with rigid elements. Finite element models for both configurations are shown in Figures 7 through 11.

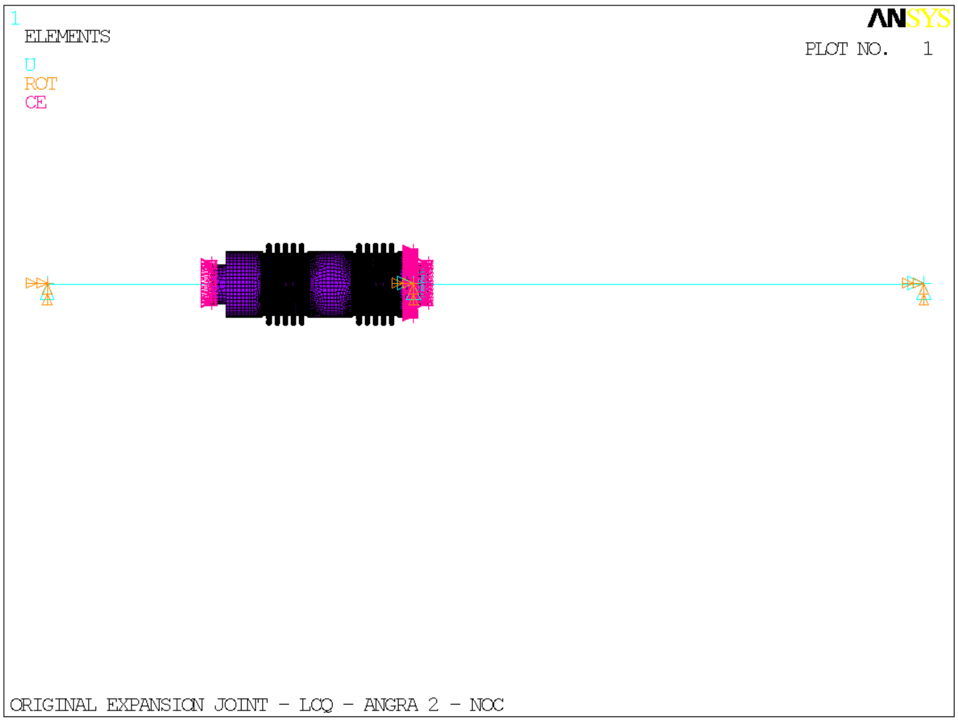

Figure 7- Original expansion joint

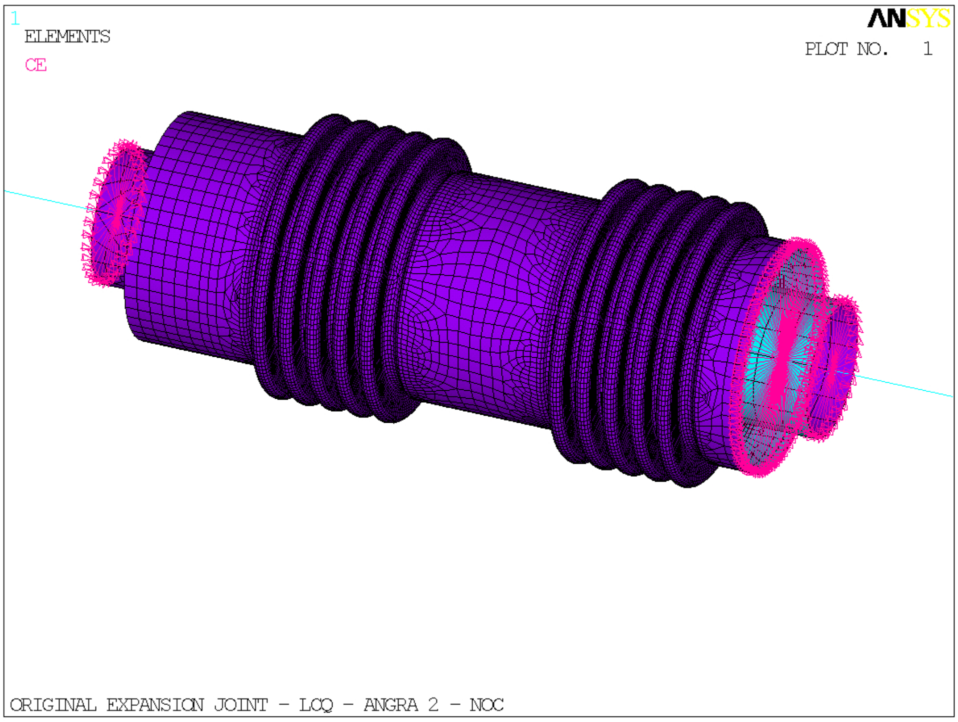

Figure 8- Original expansion joint. The transition between shell and bar elements with rigid elements

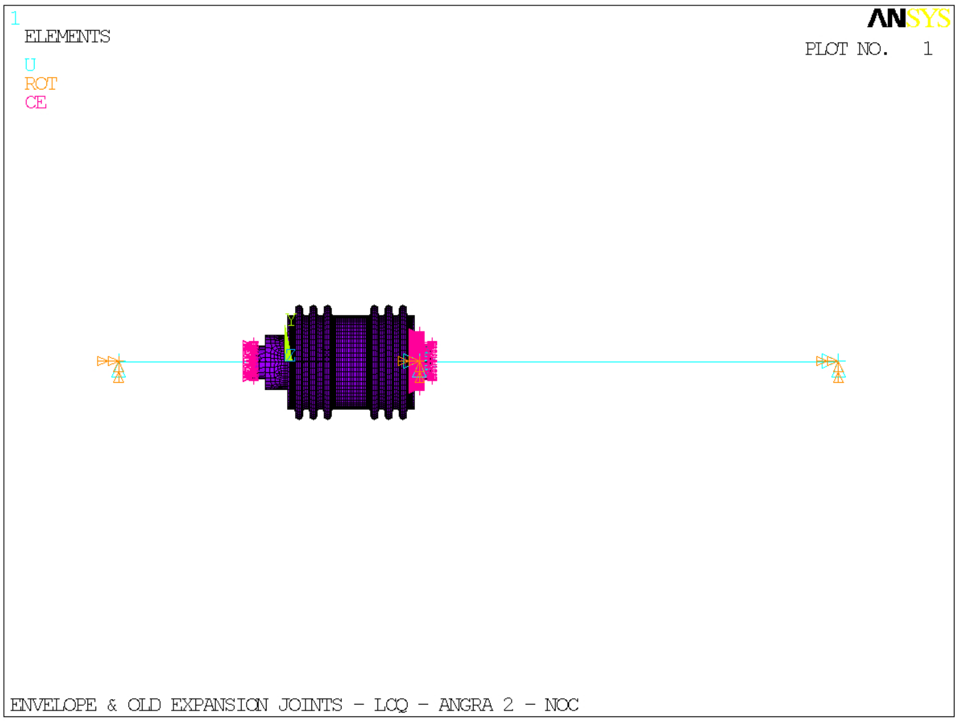

Figure 9- Original and overlapping expansion joints

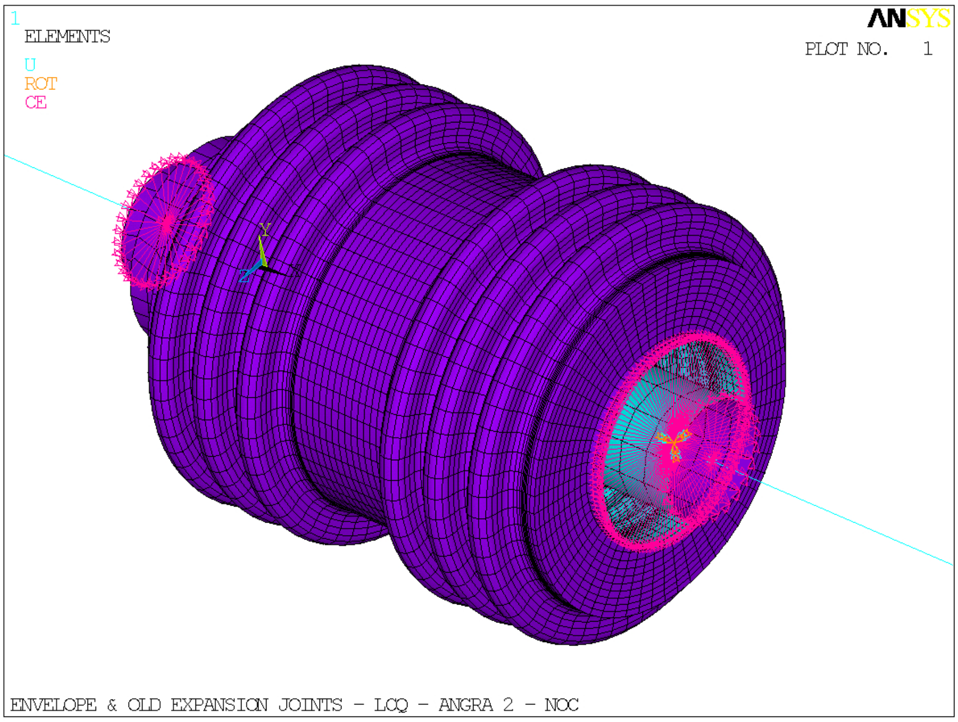

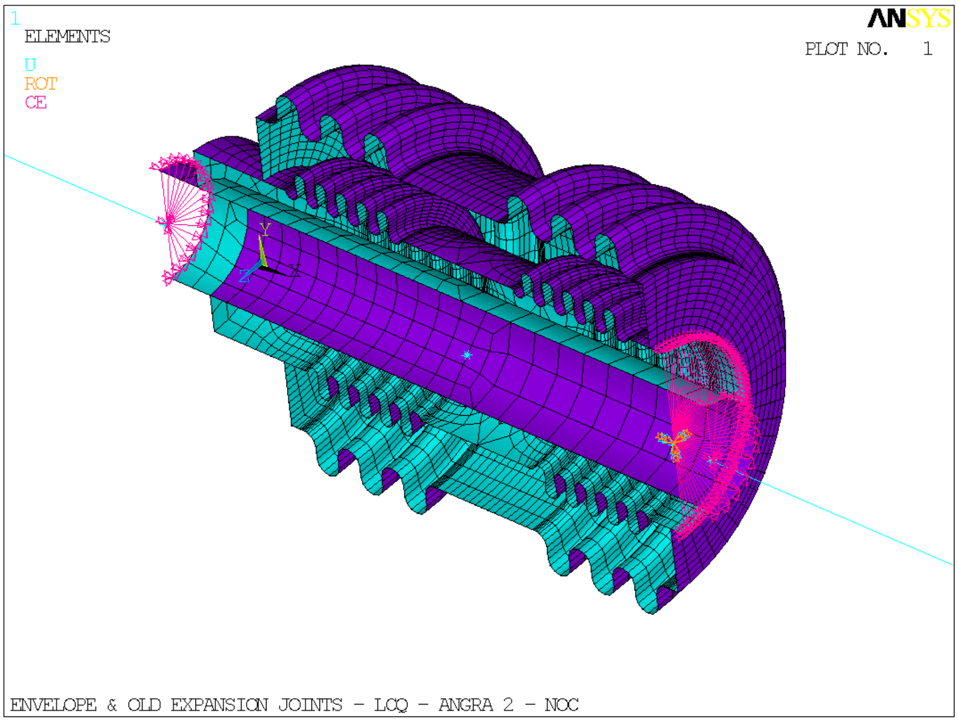

Figure 10 – Original expansion joint and overlapping joint (general and sectional views). The transition between shell and bar elements with rigid elements

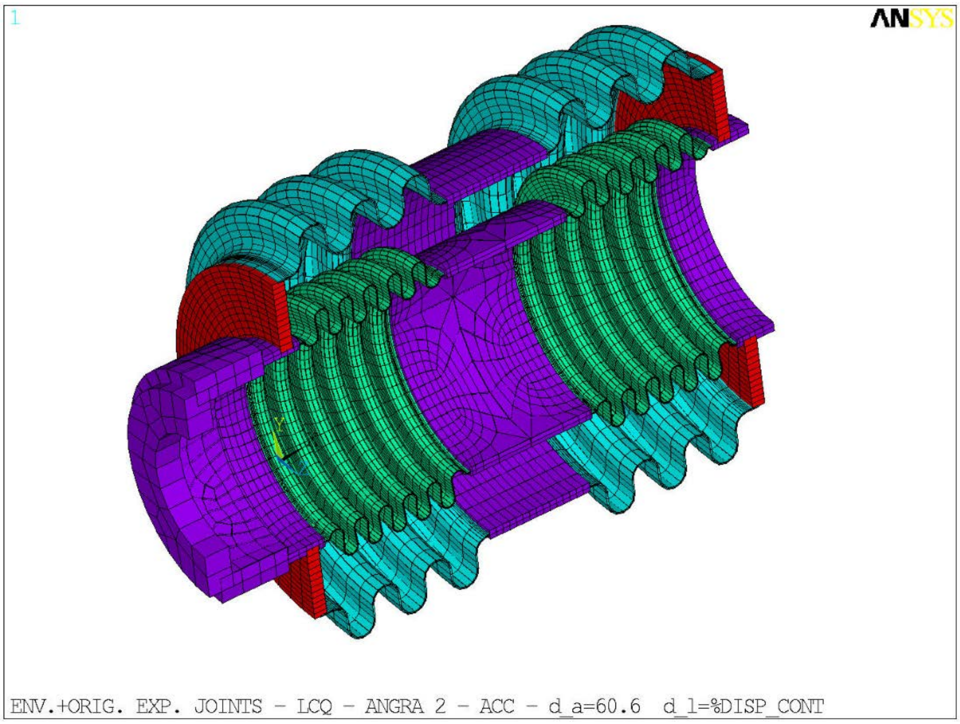

Figure 11- Sectional view and thickness of the original and overlapping expansion joints

3.1 Material properties

The original and overlapping joints are constructed with stainless steel X10CrNiNb18 9 (1.4550). The mechanical properties obtained from DIN 17440 07/85 and MTS 107.01.R2 for the various operating temperatures are shown in Table 1, with R_m tensile strength, $R_{p0.2}$, and $R_{p1.0}$ the yield limits at 0.2% and 1.0% of strain, S_m the intensity of design stresses as defined in the ASME Code, E the modulus of elasticity and α the coefficient of thermal expansion.

Table 1 - Properties of steel X10CrNiNb18 9 (1.4550)

Temperature (°C)	Rm (MPa)	Rp 0.2 (MPa)	Rp 1.0 (MPa)	Sm (MPa)	E (MPa)	α $\times10^{-6}$ (°C^{-1})
20	510	205,00	240,00	160,00	2,00000E+05	16
30	-	201,50	236,38	157,58	1,99250E+05	16
80	-	184,00	218,25	145,50	1,95500E+05	16
116	-	173,80	206,20	137,47	1,92720E+05	16

The stress versus strain curve for elastoplastic analysis is determined by the Ramberg-Osgood equation, whose plastic portion is given in the form

$$\frac{\varepsilon}{\varepsilon_o} = \alpha\left(\frac{\sigma}{\sigma_o}\right)^n \quad (1)$$

with σ the actual stress, σ_o the reference stress, usually the yield limit, ε and ε_o the actual and reference plastic deformations, this last equal to σ_o/E. The α and n parameters are material constants obtained by the best adjustment of the real stress-strain curve obtained from the tensile test.

The stress-strain relationships for the material with the characteristics of Table 1 at temperatures of 30°C, 80°C, and 116°C are shown in Figure 12.

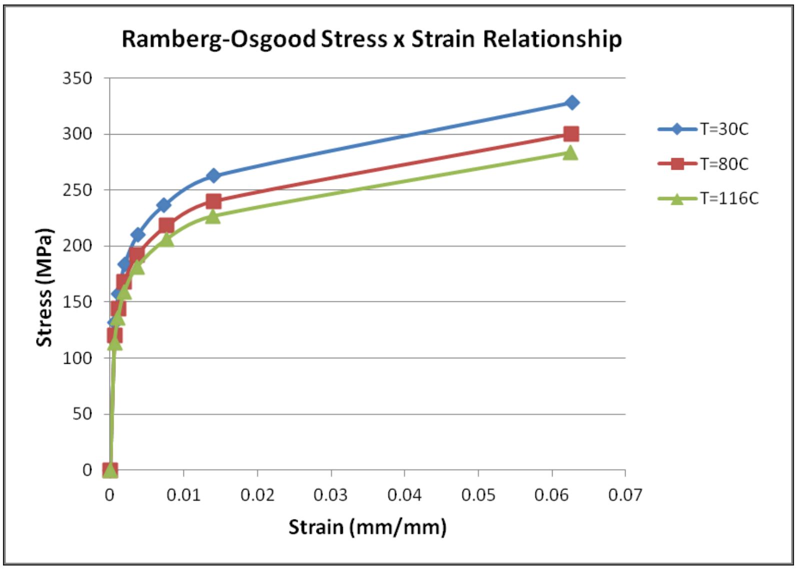

Figure 12 – Stress-strain curves for steel X10CrNiNb18 9 (1.4550)

3.2 Boundary conditions

Because the expansion joint located in the reactor building is anchored at both ends, one at the fixed point and the other welded on containment, Figure 2, movements are prevented in all directions. In the annulus, the joint is welded to containment at one end and guided (free axial displacement) through the auxiliary building on the other, Figure 3. The anchors are modeled as shown in Figure 13, which shows rigid elements coupled to the nodes of the shell elements at one end of the expansion joint to a node at the central axis of the model, which is clamped in all directions.

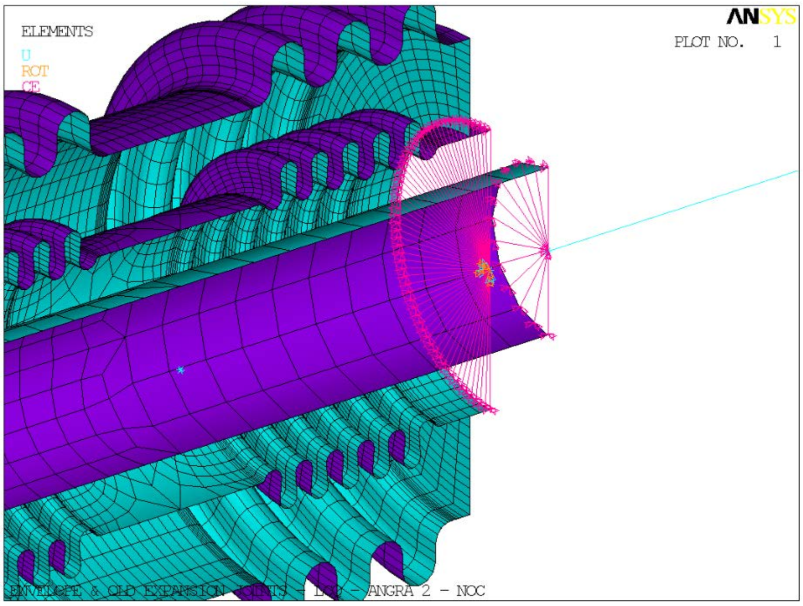

Figure 13 - Restrictions to displacements representing the anchorage in penetration in the containment

3.3 Basic loads

The load cases for the analysis of the expansion joint are the same as the original joint design and are shown in Table 2. Thermal displacements in the joint associated with the operating levels (B1+B2) are imposed by the guard pipe each time the purge system enters service. For the other levels, which depend on the movements of the containment during the pressure tests or accident events, the loading is defined by the axial and lateral displacements transmitted by penetration.

Table 2 - Description of load cases

Classification	Level	Loading Cases Description
Operation	B_1, B_2	1- Envelope normal operation/upset
Test	P	1-First Containment test
		2-Periodic Leak Tightness Containment test
Fault	S	1- LOCA corresponding to the highest pressure
		2- LOCA corresponding to the highest temperature
		3- Earthquake – SSB (SSE+BWP) – Safe Shutdown Earthquake + Burst Pressure Wave

Table 3 summarizes data taken from IWKA reports, and represents all load cases considered, inside (UJA-reactor building) and outside (UJB-annulus building) containment, in the original design of the expansion joints. The columns list for each load level the temperature, pressure range (pi=inside pressure, po=outside pressure), axial (δa), and lateral (δl) displacements respectively. The highlighted rows represent the envelope loading conditions for each load case. It is important to note that the load case P1 (First Containment Integrity and Leakage test) will not be considered in this analysis because it is performed only at the commissioning phase of the plant and therefore will not be repeated.

Table 3 – Load cases for the expansion joints

			UJA (Reactor Building)				UJB (Annulus Building)			
			p (bar)		δa (mm)	δl (mm)	p (bar)		δa (mm)	δl (mm)
	T (C)	Cicles	po	pi			po	pi		
B1+B2	80	3312	-0.005	3.0	-3.1	0.0	0.0	3.0	12.8	0.0
P1	30	1	6.2	0.0	-7.3	12.2	0.0	0.0	-39.6	22.6
P1	30	1	6.2	0.0	39.6	7.3	0.0	0.0	7.3	12.2
P2	30	15	0.5	0.0	-19.0	1.8	0.0	0.0	-21.5	1.8
P2	30	15	0.5	0.0	-21.5	0.9	0.0	0.0	19.0	0.9
S1	80	1	4.6	3.0	44.0	16.8	0.0	3.0	-34.0	16.8
S2	116	1	2.2	3.0	60.6	8.4	0.0	3.0	-49.8	8.4
S3	80	3	-0.005	3.0	0.0	0.5	0.0	3.0	0.0	0.5
S3	80	3	-0.005	3.0	5.9	0.5	0.0	3.0	15.6	0.5

The internal pressure for the original expansion joint is considered applied in the volume between the expansion joint and the guard pipe. For the overlapping expansion joint the internal pressure is applied in the volume between the overlapping expansion joint and the guard pipe once this case considers that the original expansion joint is no longer tight, and the overlapping expansion joint will perform its function. Table 4 shows the envelope loading conditions for the joints located in the reactor building and annulus.

Table 4 – Envelope Loading Conditions for each load case for the expansion joints

	T (C)	p	δa (mm)	δl (mm)
B1+B2	80	3.005(i)	12.8	0
P2	30	0.5(o)	-21.5	1.8
S1	80	4.6(o)	44	16.8
S2	116	3.0(i)	60.6	8.4
S3	80	3.005(i)	15.6	0.5

4 Results of the analysis

The methodology adopted here is to apply the loadings from the original design to the two finite element models, one for the original expansion joint and the other for the overlapping plus original joint. Thus, one can compare the stresses and deformations of each case and, from there, evaluate the changes that the modification introduces in the design configuration.

The elastic linear analysis for the operating conditions (B1+B2) is conducted assuming two load cases acting separately: i) internal pressure; ii) thermal displacement transmitted by the guard pipe. The respective stress intensities, calculated by the Tresca criterion, are determined along the path shown in Figure 14, created to represent important quantities in the two finite element models.

The stress intensity due to internal pressure in both models is calculated for the upper (TOP), middle (MIDDLE), and lower (BOTTOM) fibers, the first case is presented in

Figure 15. The meridional and circumferential stresses in a convolution are obtained in these three fibers, with the result for the upper fiber indicated in Figure 16.

The stress intensity for the upper fiber caused by the thermal displacement induced by the guard pipe for the operating condition (B1+B2) is illustrated in Figure 17, with the meridional and circumferential stresses in a convolution presented in Figure 18. Additionally, Figure 19 shows the stress intensity and deformations for thermal displacement along with a convolution for the overlapping plus original expansion joint.

An elastoplastic analysis is performed for the other loading conditions (Test-P2, LOCA-S1 and S2, and SSB-S3). The stresses and deformations in the two finite element models are obtained by simulating the properties of steel in the plastic phase with Eq. (1) and considering the material properties of Table 1.

First, the stress intensity for the upper, middle, and lower fibers for the two models in the P2-Test condition is calculated. According to Table 4, initially, the external pressure of 0.5 bar is applied and then the displacements of the containment in the axial and lateral directions, whose values are 21.5 mm and 1.8 mm, respectively. The meridional and circumferential stresses for the fibers along a convolution path and their strains (total and plastic strains) are also determined. Because of the available space, the results are shown in the table in the next section and are not plotted.

Figure 20 shows the stress intensity in the three fibers for the LOCA-S1 load case (maximum external pressure). According to Table 4, the internal pressure of 3.0 bar is applied, then the external pressure of 4.6 bar, and, finally, the axial and lateral displacements of the containment, equal to 44.0 and 16.8 mm, respectively. The meridional and circumferential stresses for the fibers along a convolution are indicated in Figure 21 and the total and plastic deformations in these directions are shown in Figure 22.

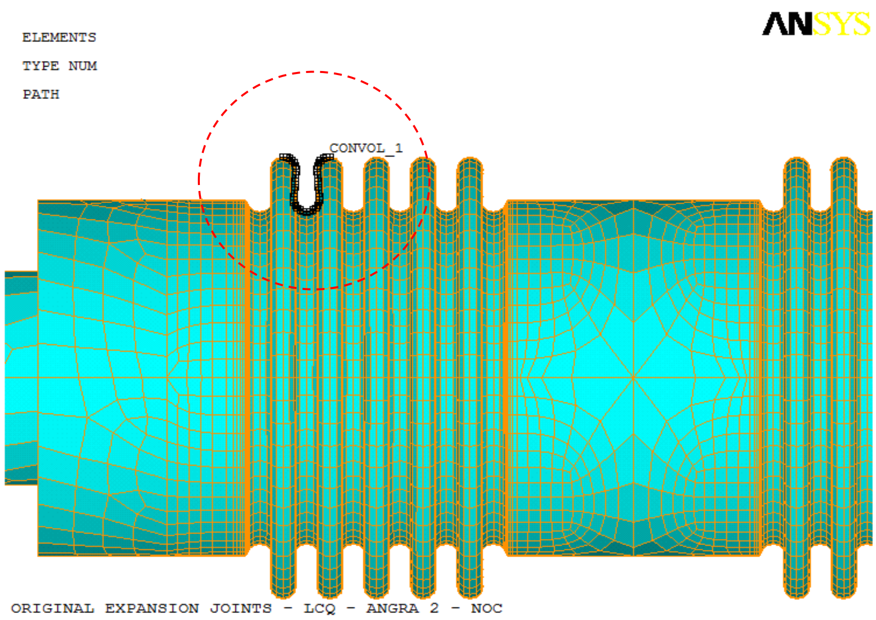

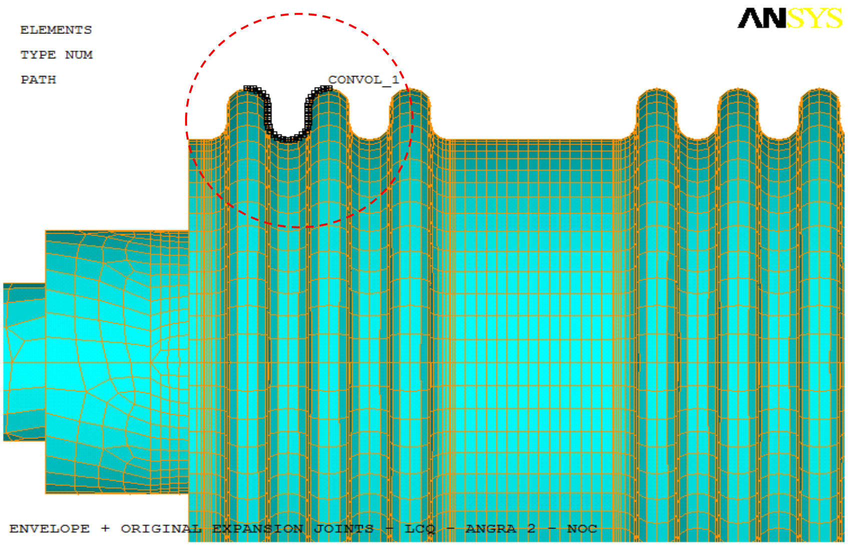

Figure 14 – Path (CONVOL_1) used to represent the meridional and circumferential stresses

The determination of the stress intensity, meridional and circumferential stresses, and total and plastic strains for the LOCA-S2 load case (maximum temperature) is made initially with the application of the internal pressure of 3.0 bar and then with axial displacements of 60.6 mm and lateral displacements of 8.4 mm imposed by containment. These same amounts are found for the SSB-S3 case when the safe shutdown earthquake and pressure waves (SSE+BPW) are superimposed. First, the internal pressure of 3.005 bar is applied, and then the displacements of the containment in the axial directions, equal to 15.6 mm, and lateral, equal to 0.5 mm. The results are in the tables shown in the next section.

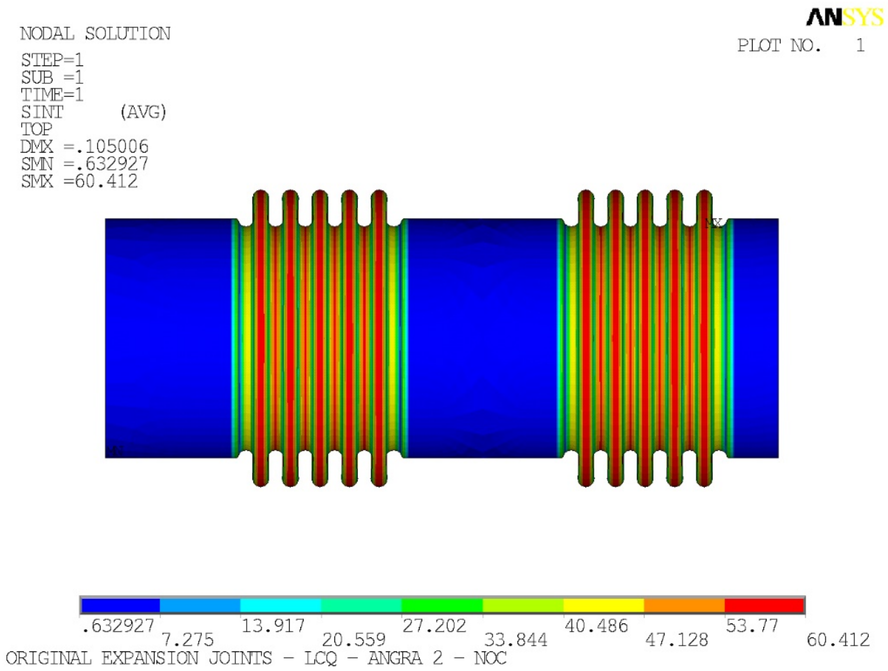

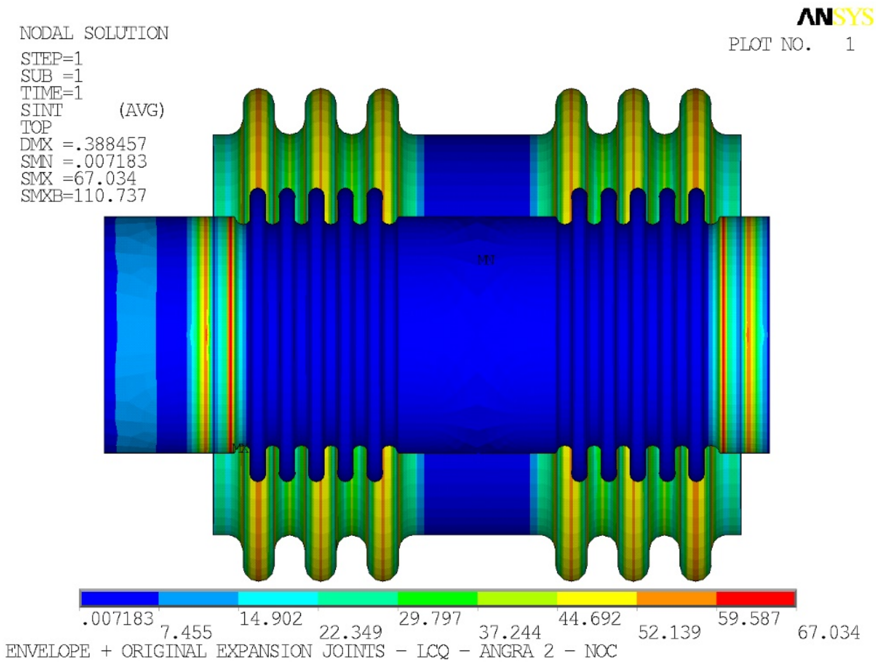

Figure 15– Original & Overlapping + Original Expansion Joints- Stress Intensity –TOP – Load case B1+B2 – Internal Pressure

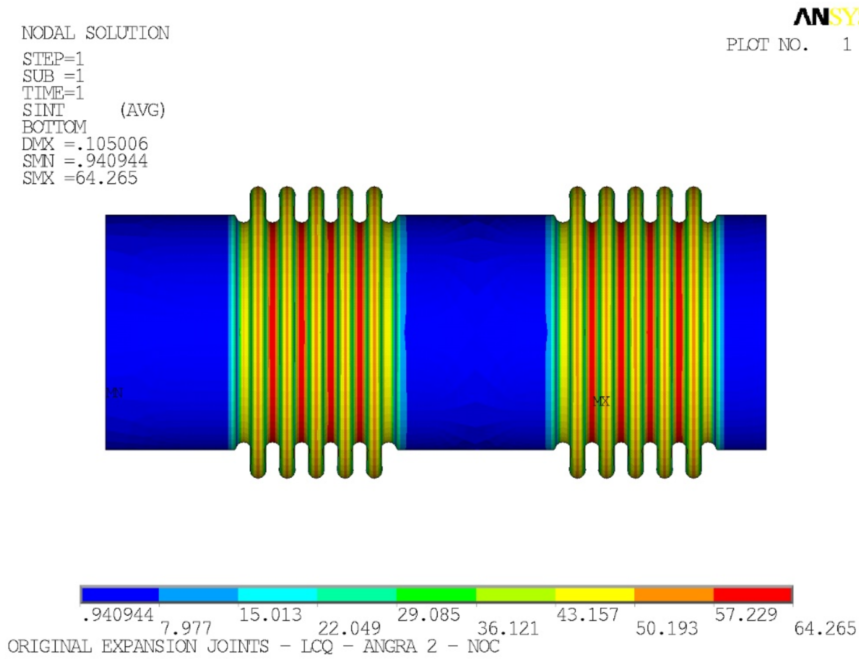

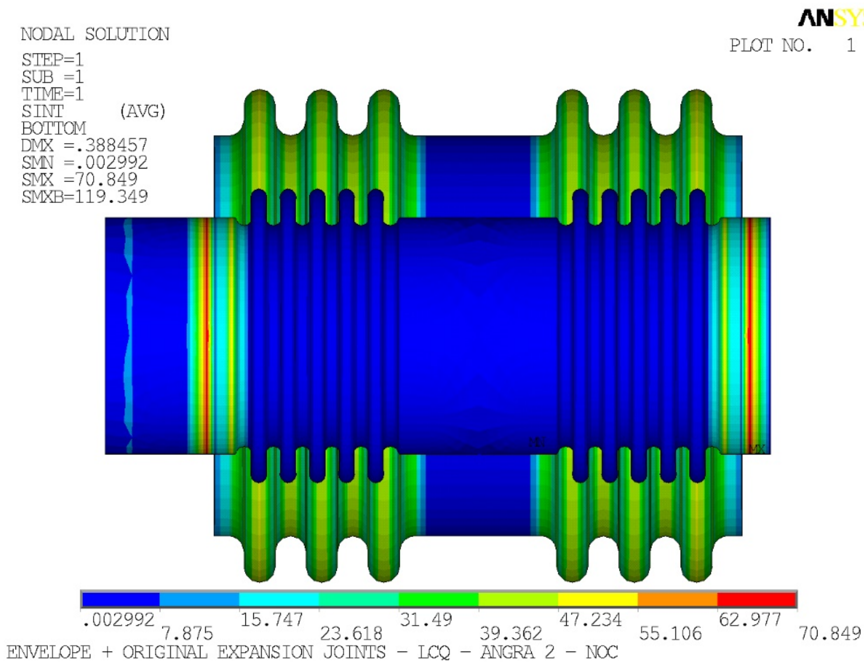

Figure 16– Original & Overlapping + Original Expansion Joints - Stress Intensity –BOTTOM – Load case B1+B2– Internal Pressure

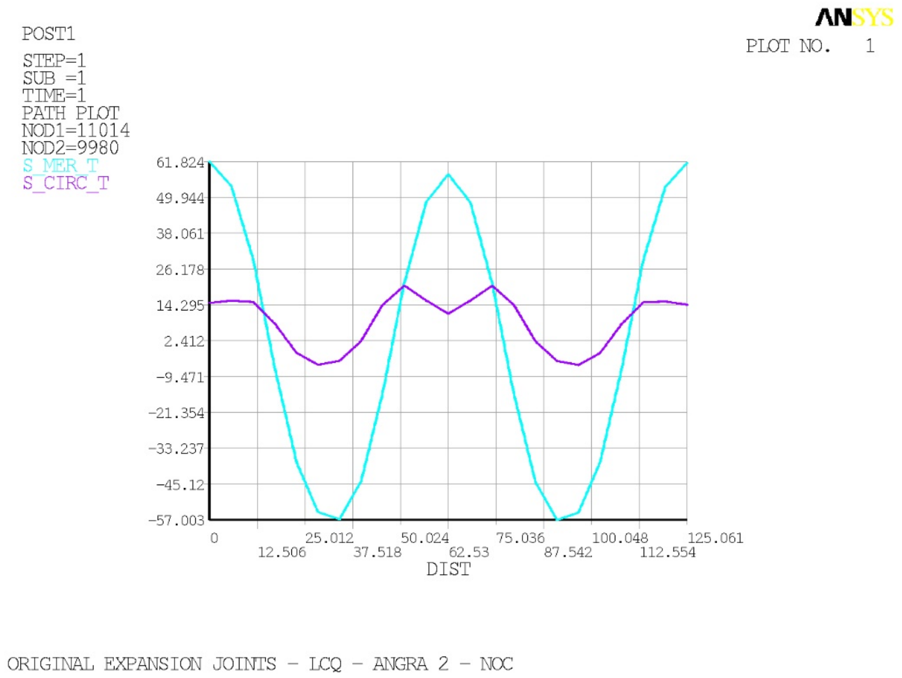

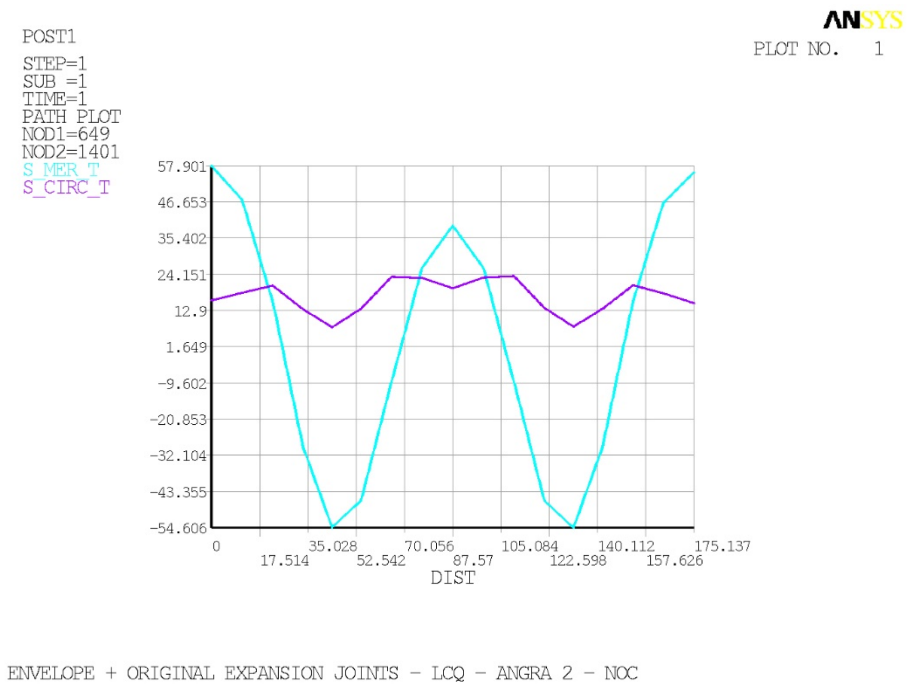

Figure 17– Original & Overlapping + Original Expansion Joints - Meridional and Circumferential Stress – TOP – Load case B1+B2– Internal Pressure

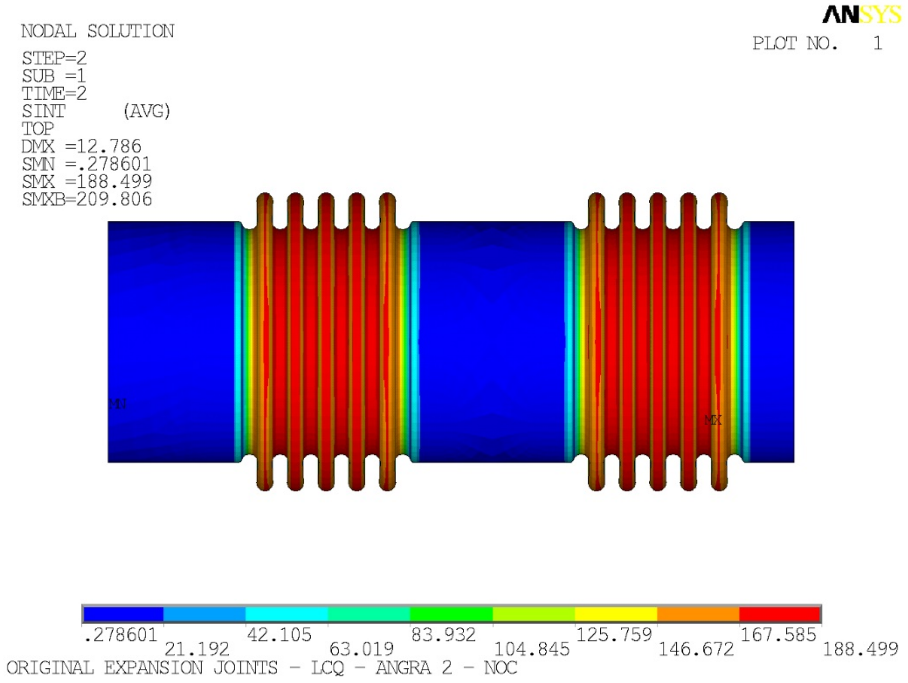

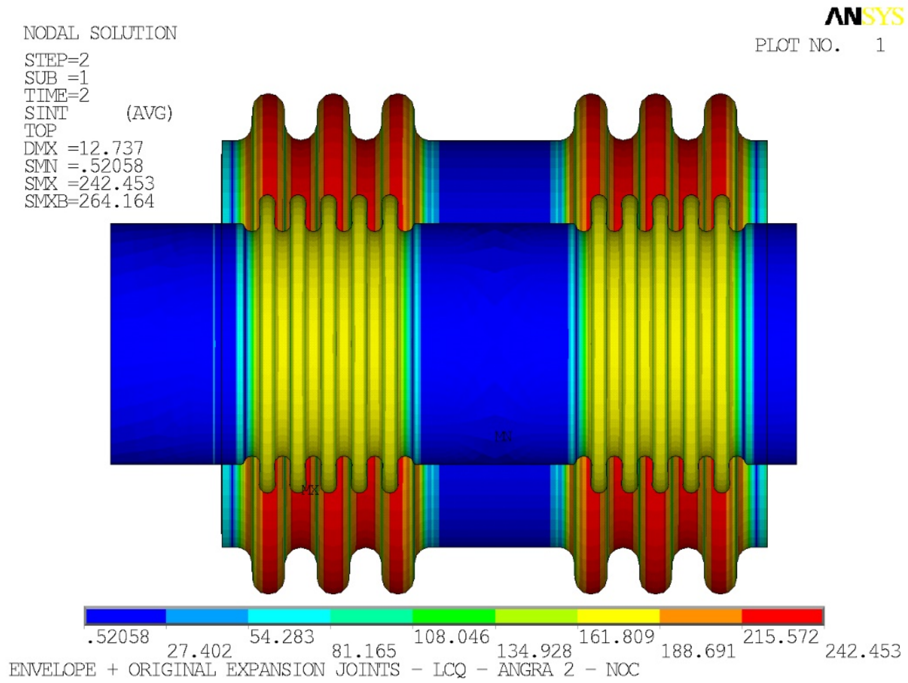

Figure 18– Original & Overlapping + Original Expansion Joints- Stress Intensity –TOP – Load case B1+B2 – Thermal Displacement

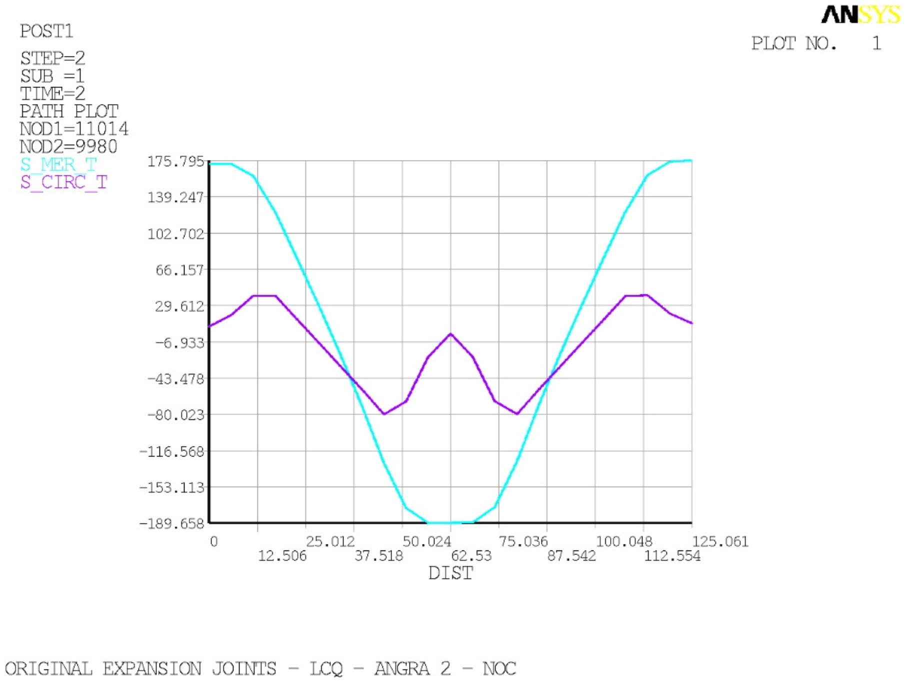

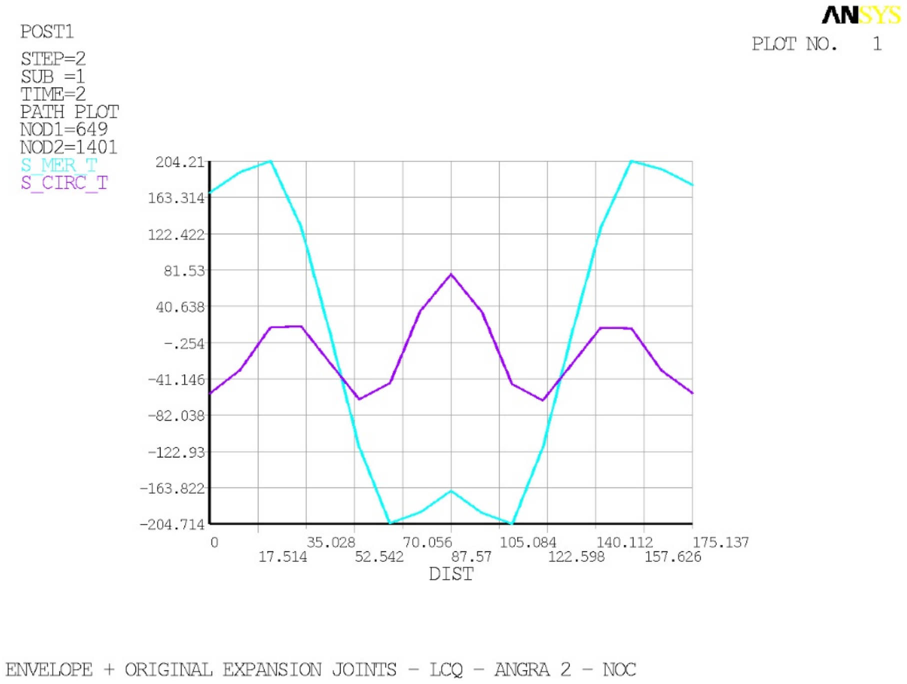

Figure 19– Original & Overlapping + Original Expansion Joints - Meridional and Circumferential Stress – TOP – Load case B1+B2– Thermal Displacement

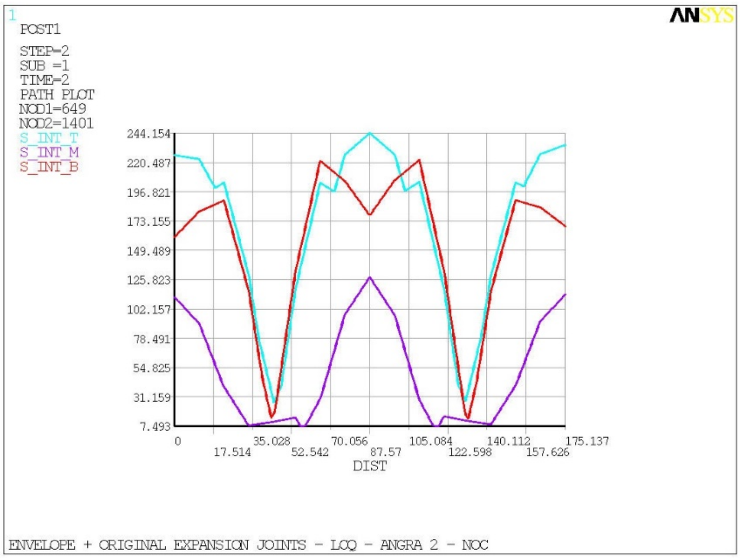

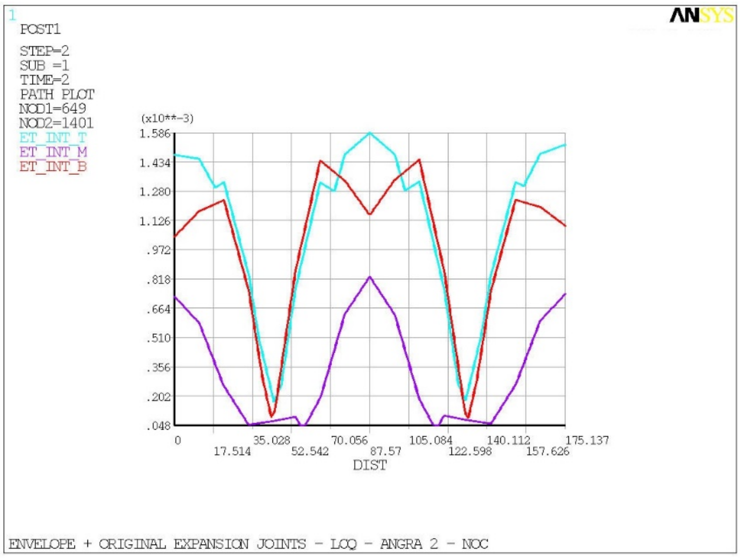

Figure 20– Overlapping + Original Expansion Joints - Stress Intensity and Strain Intensity – TOP, MIDDLE, BOTTOM – Load case B1+B2– Thermal Displacement

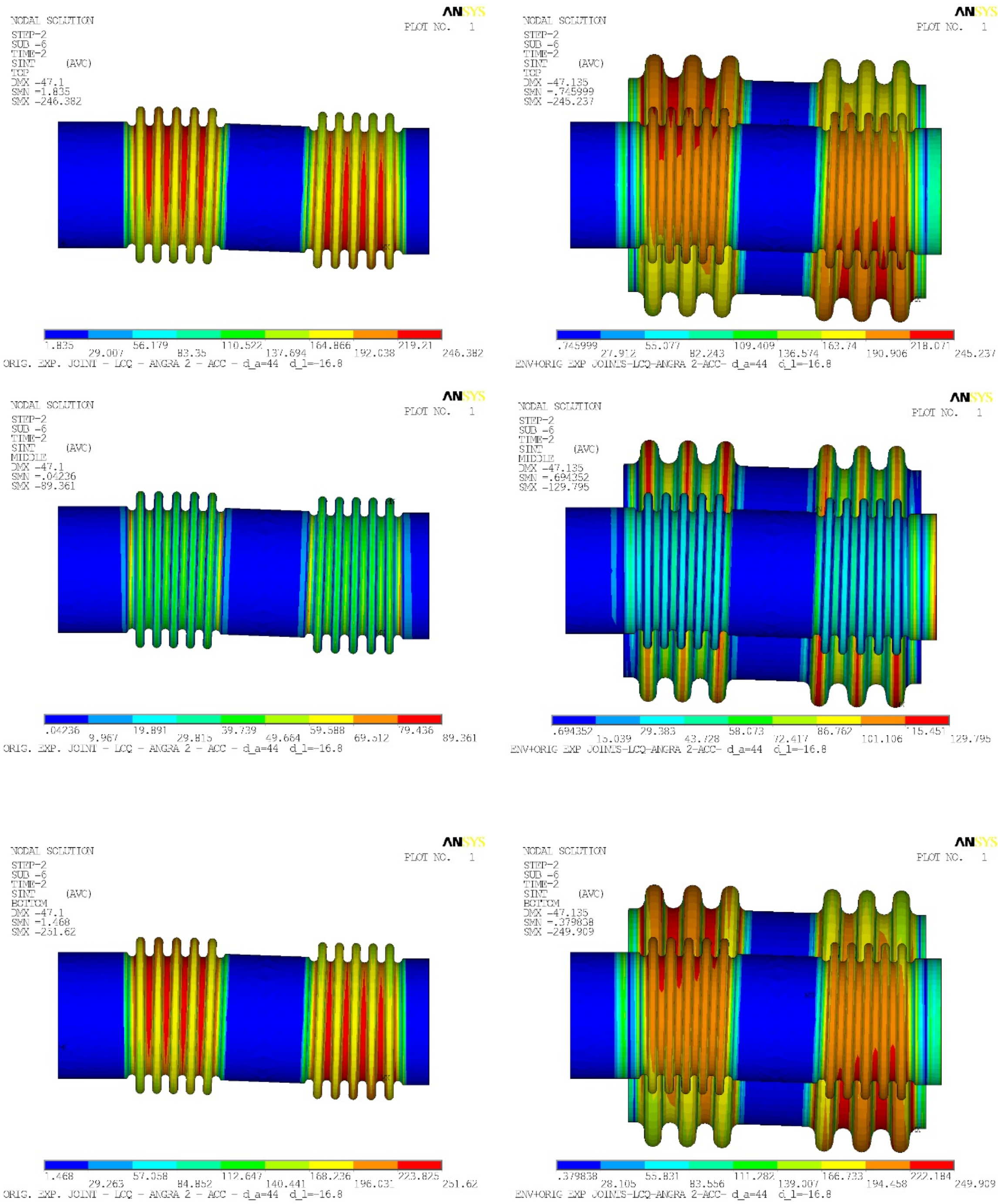

Figure 21– Original & Overlapping + Original Expansion Joints - Stress Intensity– TOP, MIDDLE & BOTTOM – Load case S1 – Internal Pressure Followed by External Pressure + Containment Axial and Lateral Displacements

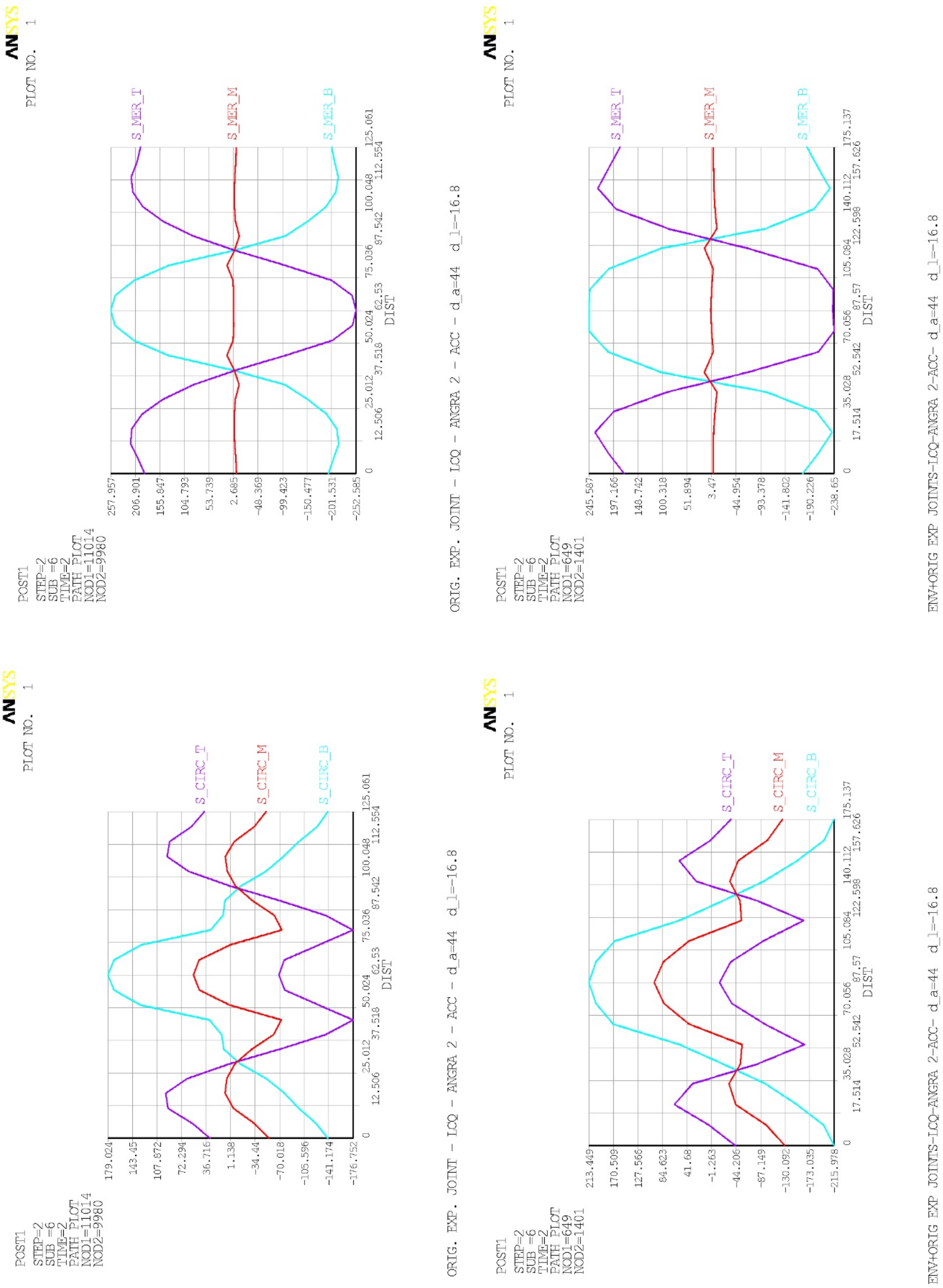

Figure 22– Original & Overlapping + Original Expansion Joints - Circumferential and Meridional Stresses– TOP, MIDDLE & BOTTOM – Load case S1 – Internal Pressure Followed by External Pressure + Containment Axial and Lateral Displacements

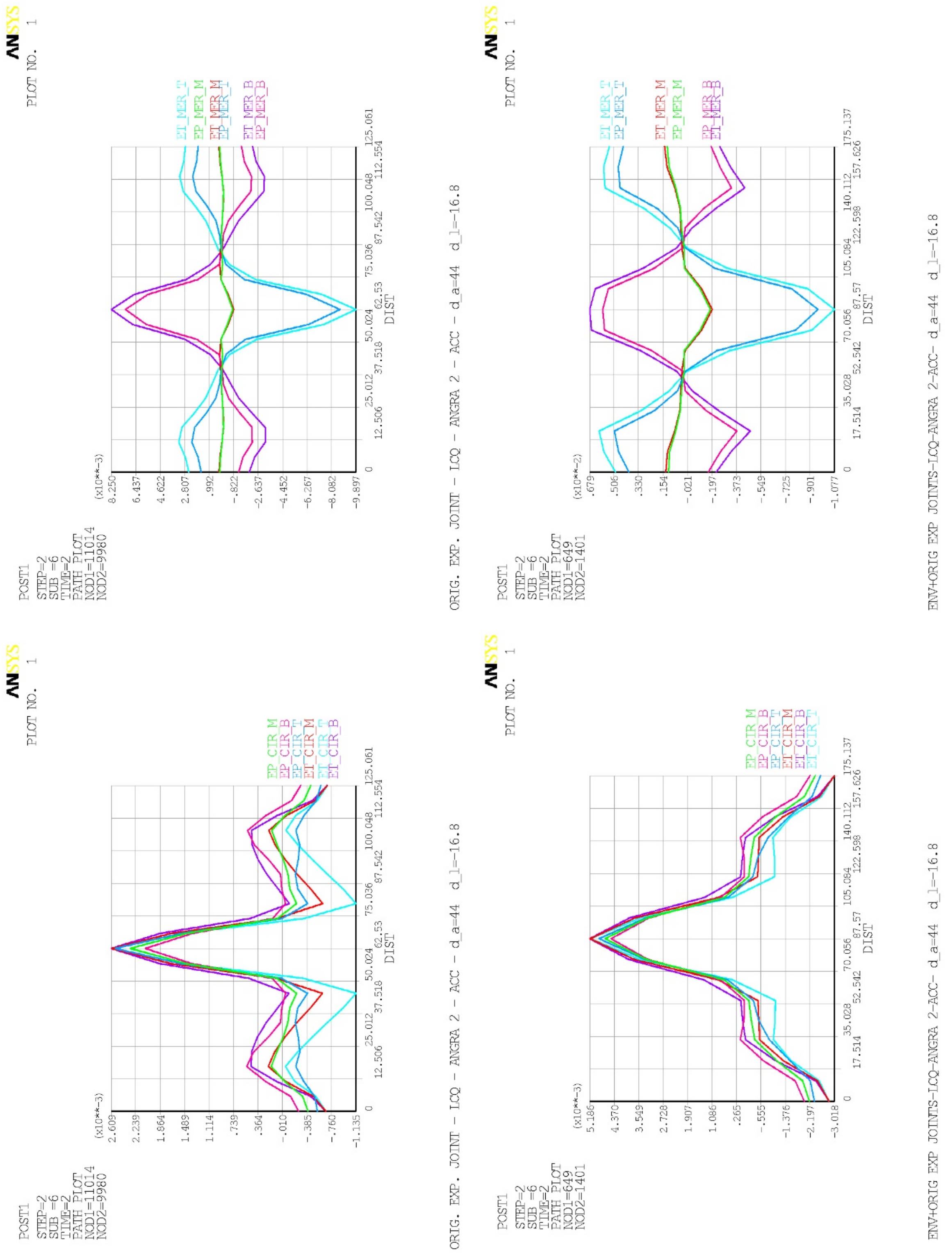

Figure 23– Original & Overlapping + Original Expansion Joints - Circumferential and Meridional Total Strains and Plastic Strains– TOP, MIDDLE & BOTTOM – Load case S1 – Internal Pressure Followed by External Pressure + Containment Axial and Lateral Displacements

5 Stress and fatigue analysis

The stress analysis of the overlapping expansion joint for the operation case (B1+B2) was performed considering the rules of the ASME Code Section III NB-3200. Although this type of verification has not been adopted for the original joint, since the usual is to design it according to the criteria of AD- 2000/B13, here we opted for detailed stress analysis. This alternative gave greater consistency to the structural design of the new piece and facilitated its approval with regulatory agencies in Brazil and Germany. For the other load cases, the qualification of the overlapping joint was by comparison between the results found in its analysis and the original joint.

Expansion joints are used to add flexibility to piping systems. They must withstand internal pressure and, at the same time, be able to absorb, for example, thermal movements. The latter are typically in the form of axial deflections or rotations and, in some cases, lateral displacements at the extremities. Because displacements depend on the number of times the system heats up and cools, the joint should be designed against fatigue.

Joints when requested by internal pressure are subjected to circumferential and meridional stresses. These stresses are called primary, a term used by the ASME code to describe the stresses arising from the external loading, which must satisfy the equilibrium conditions, and which are not self-limiting, that is, once a limit value is reached, plastic flow or collapse occurs. Primary stresses differ from secondary stresses, which in turn have their magnitude reduced as the piece deforms. As secondary stresses are self-limiting, they cause fatigue but do not contribute to the fracture.

In general, expansion joints are analyzed in an elastic regime, even when subjected to high stresses. This is possible because a significant portion of the stresses are secondary and therefore can exceed the yield limit without material failure. The fatigue curves of the ASME Section III code, for example, show values that exceed yield resistance and are therefore deformation curves versus the number of cycles. Thus, although the stress calculated in the elastic regime is not real, it serves as a measure of the strain imposed on the component.

Tables 5 through 10 summarize the results for each of the load cases analyzed in the previous section. The terms that appear in the columns of the tables are identified as:

S_CIR_MAX	Maximum circumferential stress (MPa)
S_CIR_MIN	Minimum circumferential stress (MPa)
S_MER_MAX	Maximum meridional stress (MPa)
S_MER_MIN	Minimum meridional stress (MPa)
S_INT_MAX	Maximum stress intensity (MPa)
ET_CIR_MAX	Maximum circumferential total strain (%)
ET_CIR_MIN	Minimum circumferential total strain (%)
ET_MER_MAX	Maximum meridional total strain (%)
ET_MER_MIN	Minimum meridional total strain (%)
ET_INT_MAX	Maximum total strain intensity (%)
EP_CIR_MAX	Maximum circumferential plastic strain (%)
EP_CIR_MIN	Minimum circumferential plastic strain (%)
EP_MER_MAX	Maximum meridional plastic strain (%)
EP_MER_MIN	Minimum meridional plastic strain (%)

Table 5 – Summary of the Maximum/Minimum Circumferential and Meridional Stresses, Maximum Stress and Strain Intensity for Load case B1+B2 - Internal Pressure

	ORIGINAL EXPANSION JOINT			
	S_CIR_MAX(MPa)	S_CIR_MIN(MPa)	S_MER_MAX(MPa)	S_MER_MIN(MPa)
TOP	20.711	-5.62	61.824	-57.003
MID	15.228	-6.924	3.588	-4.077
BOT	29.509	-25.246	57.044	-65.747
	S_INT_MAX(MPa)	ET_INT_MAX(%)		
TOP	61.824	0.04		
MID	16.22	0.011		
BOT	65.747	0.043		

	OVERLAPPING+ORIGINAL EXPANSION JOINT			
	S_CIR_MAX(MPa)	S_CIR_MIN(MPa)	S_MER_MAX(MPa)	S_MER_MIN(MPa)
TOP	23.598	7.716	57.902	-54.606
MID	26.635	-0.529	3.891	-3.833
BOT	42.859	-16.611	55.725	-50.12
	S_INT_MAX(MPa)	ET_INT_MAX(%)		
TOP	62.501	0.041		
MID	26.963	0.018		
BOT	55.725	0.036		

Table 6 – Summary of the Maximum/Minimum Circumferential and Meridional Stresses, Maximum Stress and Strain Intensity for Load case B1+B2 - Thermal Displacement

	ORIGINAL EXPANSION JOINT			
	S_CIR_MAX(MPa)	S_CIR_MIN(MPa)	S_MER_MAX(MPa)	S_MER_MIN(MPa)
TOP	39.819	-80.091	175.795	-189.658
MID	58.382	-42.908	3.969	0.507
BOT	115.547	-94.224	197.516	-170.681
	S_INT_MAX(MPa)	ET_INT_MAX(%)		
TOP	190.481	0.124		
MID	58.382	0.038		
BOT	197.516	0.128		

	OVERLAPPING+ORIGINAL EXPANSION JOINT			
	S_CIR_MAX(MPa)	S_CIR_MIN(MPa)	S_MER_MAX(MPa)	S_MER_MIN(MPa)
TOP	76.667	-65.608	204.21	-204.714
MID	127.792	-109.596	8.858	4.174
BOT	178.917	-161.994	222.42	-189.968
	S_INT_MAX(MPa)	ET_INT_MAX(%)		
TOP	244.154	0.159		
MID	127.792	0.083		
BOT	222.42	0.145		

Table 7 – Summary of the Maximum/Minimum Circumferential and Meridional Stresses and Strains for Load case P2

	ORIGINAL EXPANSION JOINT			
	S_CIR_MAX(MPa)	S_CIR_MIN(MPa)	S_MER_MAX(MPa)	S_MER_MIN(MPa)
TOP	109.12	-57.001	197.901	-199.475
MID	41.275	-54.978	1.248	-5.916
BOT	123.347	-139.8	201.49	-207.454
	ET_CIR_MAX(%)	ET_CIR_MIN(%)	ET_MER_MAX(%)	ET_MER_MIN(%)
TOP	0.041	-0.057	0.2	-0.191
MID	0.041	-0.057	0.019	-0.02
BOT	0.041	-0.057	0.151	-0.162
	EP_CIR_MAX(%)	EP_CIR_MIN(%)	EP_MER_MAX(%)	EP_MER_MIN(%)
TOP	0.033	-0.042	0.106	-0.098
MID	0.021	-0.03	0.013	-0.015
BOT	0.009	-0.018	0.068	-0.079

	OVERLAPPING+ORIGINAL EXPANSION JOINT			
	S_CIR_MAX(MPa)	S_CIR_MIN(MPa)	S_MER_MAX(MPa)	S_MER_MIN(MPa)
TOP	85.529	-35.008	193.348	-194.055
MID	92.504	-111.072	2.866	-8.799
BOT	177.763	-189.879	199.447	-203.317
	ET_CIR_MAX(%)	ET_CIR_MIN(%)	ET_MER_MAX(%)	ET_MER_MIN(%)
TOP	0.112	-0.135	0.233	-0.239
MID	0.112	-0.135	0.05	-0.052
BOT	0.111	-0.135	0.145	-0.16
	EP_CIR_MAX(%)	EP_CIR_MIN(%)	EP_MER_MAX(%)	EP_MER_MIN(%)
TOP	0.08	-0.093	0.142	-0.144
MID	0.066	-0.08	0.037	-0.039
BOT	0.051	-0.068	0.069	-0.085

Table 8 – Summary of the Maximum/Minimum Circumferential and Meridional Stresses and Strains for Load case S1

	ORIGINAL EXPANSION JOINT			
	S_CIR_MAX(MPa)	S_CIR_MIN(MPa)	S_MER_MAX(MPa)	S_MER_MIN(MPa)
TOP	95.2	-176.752	216.864	-252.585
MID	54.979	-73.253	16.233	-9.503
BOT	179.024	-140.07	257.957	-216.651
	ET_CIR_MAX(%)	ET_CIR_MIN(%)	ET_MER_MAX(%)	ET_MER_MIN(%)
TOP	0.258	-0.114	0.324	-0.99
MID	0.26	-0.07	0.027	-0.082
BOT	0.261	-0.07	0.825	-0.316
	EP_CIR_MAX(%)	EP_CIR_MIN(%)	EP_MER_MAX(%)	EP_MER_MIN(%)
TOP	0.255	-0.06	0.227	-0.871
MID	0.232	-0.044	0.02	-0.075
BOT	0.209	-0.029	0.721	-0.22

	OVERLAPPING+ORIGINAL EXPANSION JOINT			
	S_CIR_MAX(MPa)	S_CIR_MIN(MPa)	S_MER_MAX(MPa)	S_MER_MIN(MPa)
TOP	63.697	-164.054	233.535	-238.65
MID	99.05	-129.686	17.622	-7.141
BOT	213.449	-215.978	245.587	-234.766
	ET_CIR_MAX(%)	ET_CIR_MIN(%)	ET_MER_MAX(%)	ET_MER_MIN(%)
TOP	0.516	-0.301	0.613	-1.077
MID	0.517	-0.302	0.143	-0.199
BOT	0.519	-0.302	0.68	-0.473
	EP_CIR_MAX(%)	EP_CIR_MIN(%)	EP_MER_MAX(%)	EP_MER_MIN(%)
TOP	0.488	-0.255	0.503	-0.959
MID	0.467	-0.237	0.124	-0.186
BOT	0.447	-0.22	0.587	-0.376

Table 9 – Summary of the Maximum/Minimum Circumferential and Meridional Stresses and Strains for Load case S2

	ORIGINAL EXPANSION JOINT			
	S_CIR_MAX(MPa)	S_CIR_MIN(MPa)	S_MER_MAX(MPa)	S_MER_MIN(MPa)
TOP	86.096	-153.483	223.175	-227.011
MID	57.223	-42.412	10.927	-0.473
BOT	168.3	-150.65	230.614	-223.124
	ET_CIR_MAX(%)	ET_CIR_MIN(%)	ET_MER_MAX(%)	ET_MER_MIN(%)
TOP	0.215	-0.134	0.613	-0.753
MID	0.216	-0.134	0.066	-0.08
BOT	0.217	-0.134	0.593	-0.481
	EP_CIR_MAX(%)	EP_CIR_MIN(%)	EP_MER_MAX(%)	EP_MER_MIN(%)
TOP	0.208	-0.134	0.508	-0.644
MID	0.186	-0.112	0.06	-0.072
BOT	0.165	-0.09	0.499	-0.389

	OVERLAPPING+ORIGINAL EXPANSION JOINT			
	S_CIR_MAX(MPa)	S_CIR_MIN(MPa)	S_MER_MAX(MPa)	S_MER_MIN(MPa)
TOP	54.912	-134.506	221.804	-217.793
MID	111.14	-92.424	8.216	-1.778
BOT	210.961	-199.017	222.535	-220.61
	ET_CIR_MAX(%)	ET_CIR_MIN(%)	ET_MER_MAX(%)	ET_MER_MIN(%)
TOP	0.482	-0.376	0.838	-0.893
MID	0.483	-0.376	0.195	-0.202
BOT	0.484	-0.376	0.567	-0.481
	EP_CIR_MAX(%)	EP_CIR_MIN(%)	EP_MER_MAX(%)	EP_MER_MIN(%)
TOP	0.444	-0.35	0.729	-0.786
MID	0.425	-0.328	0.18	-0.186
BOT	0.407	-0.306	0.481	-0.395

Table 10 – Summary of the Maximum/Minimum Circumferential and Meridional Stresses and Strains for Load case S3

	ORIGINAL EXPANSION JOINT			
	S_CIR_MAX(MPa)	S_CIR_MIN(MPa)	S_MER_MAX(MPa)	S_MER_MIN(MPa)
TOP	43.084	-89.158	156.929	-162.339
MID	44.265	-35.463	4.853	-1.946
BOT	110.502	-93.911	172.046	-160.585
	ET_CIR_MAX(%)	ET_CIR_MIN(%)	ET_MER_MAX(%)	ET_MER_MIN(%)
TOP	0.038	-0.026	0.116	-0.14
MID	0.038	-0.026	0.012	-0.013
BOT	0.039	-0.026	0.115	-0.092
	EP_CIR_MAX(%)	EP_CIR_MIN(%)	EP_MER_MAX(%)	EP_MER_MIN(%)
TOP	0.025	-0.015	0.04	-0.061
MID	0.017	-0.009	0.008	-0.008
BOT	0.008	-0.003	0.044	-0.024

	OVERLAPPING+ORIGINAL EXPANSION JOINT			
	S_CIR_MAX(MPa)	S_CIR_MIN(MPa)	S_MER_MAX(MPa)	S_MER_MIN(MPa)
TOP	29.829	-68.497	157.956	-158.092
MID	91.725	-80.838	7.851	-3.891
BOT	153.62	-143.882	167.866	-160.582
	ET_CIR_MAX(%)	ET_CIR_MIN(%)	ET_MER_MAX(%)	ET_MER_MIN(%)
TOP	0.087	-0.073	0.147	-0.152
MID	0.087	-0.073	0.031	-0.03
BOT	0.088	-0.073	0.109	-0.093
	EP_CIR_MAX(%)	EP_CIR_MIN(%)	EP_MER_MAX(%)	EP_MER_MIN(%)
TOP	0.05	-0.042	0.069	-0.076
MID	0.042	-0.032	0.021	-0.02
BOT	0.033	-0.023	0.045	-0.03

The permissible stresses for case B1+B2 are obtained from Table 1 and the stress limits for the corresponding temperature are those of ASME code Section III NB-3200, [1], shown in Table 11.

Table 11 – Admissible Stress for Primary and Secondary stresses

Stress Category	Admissible Stress (MPa) T=80°C
P_m = Primary Membrane	S_m=145.50
P_L+P_b = Primary Local + Bending	1.5 S_m=218.25
P+Q = Primary + Secondary	3.0 S_m=436.50

The current stresses calculated according to ASME Section III NB-3200 and the respective stress limits are compared in Table 12. It is observed that the primary and secondary stresses meet the criteria of the code.

Table 12 – Comparison between Primary and Secondary Acting Stress and Admissible Stress

Stress Category	Acting Stress (MPa) Original expansion joint	Acting Stress (MPa) Original expansion joint	Admissible Stress (MPa) T=80°C
P_m	16.2	27.0	S_m=145.50
P_L+P_b	65.7	62.5	1.5 S_m=218.25
P+Q	197.5	244.1	3.0 S_m=436.50

In fatigue analysis, only the operating conditions (B1+B2) are considered, since the number of cycles for the other conditions (P1, P2, S1, S2, S3) is very low. The stresses due to internal pressure and thermal displacements were obtained by elastic analysis and are shown in Tables 5 and 6.

Fatigue analysis is performed based on effective total strain range curves versus cycles obtained by numerous tests conducted by joint manufacturers. The AD-2000/B13 establishes the correlation

$$N = \left(\frac{10}{2.\varepsilon_{ages}}\right)^{3.45} \quad \text{for } 500 \leq N \leq 10^6 \qquad (2)$$

where N is the number of cycles to failure and ε_{ages} is the strain. The allowable number of N_{allow} cycles is

$$N_{allow} \leq \frac{N}{S_L} \quad \text{with } S_L = 5.0 \qquad (3)$$

Where S_L is a safety factor adopted for cases in which there are no fatigue test results in the installed joint, as is the situation of Angra 2.

From Table 6 the maximum total deformation intensity is $2\varepsilon_{ages}$=0.159%. As the longitudinal weld of the overlapping joint was manufactured during assembly in the field, an additional safety factor of 4 is employed. By replacing these values in the previous formula, we reach the allowable number of stress cycles N_{allow} equal to 2686 cycles.

It is noted that the calculated number is much higher than expected to occur during the remaining life of the plant. The qualification of the modified configuration for the other load cases (Test-P2, LOCA-S1 and S2, and SSB-S3) was made by comparing the results obtained for the models with the original joint and those with the overlapping joint.

Tables 7 to 10 show that even if there is an increase in plastic strain for the new configuration, these values are close to 1%, with a total strain value equal to 1.077% (load case S1).

6 Conclusions

This chapter presents the stress and fatigue analysis of the modification performed in the original expansion joint of the Angra 2 steam generator purge system. The amendment, which consisted of installing an overlapping joint capable of resisting all originally planned loads, was adopted to circumvent the problems arising from replacing the deformed joint with a new one.

Two finite element models were developed, one to simulate the original joint and the other to represent the original plus the overlapping joint. The analyses were performed under an elastic regime for the operation condition (internal pressure and thermal displacements) and elastoplastic for the test and accident cases (earthquake and LOCA).

The overlapping joint was qualified for the operation loads (B1+B2) comparing the current stresses with the limits of the ASME Code Section III NB-3200. For fatigue analysis, the AD 2000/B13 procedure was followed. For the other requests (Test-P2, LOCA-S1 and S2, and SSB-S3) the structural qualification was made by comparing the results of both models, using the value of the calculated plastic deformation.

References

ASME Section III Rules for Construction of Nuclear Power Plant Components, ASME B&P Vessel Code, American Society of Mechanical Engineers. New York, 2010.

AD 2000-MerkBlatt B13 - Single-ply bellows expansion joints.

ANSYS 12.1® - User manual.

DIN 17440 07/85 Stainless steels; technical delivery conditions for plates, hot-rolled strip, wire rods, drawn wire, bars, forgings, and semi-finished products.

MTS 107.01.R2 – Material Test Sheet

IWKA reports 501.02-300155/300156 – Bellows Design

Ramberg, W.; W. R. Osgood. Description of Stress-Strain Curves by Three Parameters. NACA TN 402, National Advisory Committee for Aeronautics, 1943.

Kraftwerk Union, Angra 2 BRA 011RSB Rohrdurchfuhrung Auslegungsblatt fur Kompensatoren ABK, V 245/134/82, Seite 13.1/13.2.

Suanno, R., Fatigue and Stress Analysis of the Bipartite Overlapping Expansion Joints of the Containment Penetration JMK05D0201 (LCQ50) – Eletronuclear internal report BQ/2/LCQ50/110114

Suanno, R., Maneschy, J.E., Francioni, M., Stress Analysis of the Bipartite Overlapping Expansion Joints of the Containment Penetration – Angra 2. Proceedings of the ASME 2012 Pressure Vessels & Piping Division Conference, PVP2012-78840, Toronto, Ontario, Canada.